CO$_2$ supercritical extraction and microencapsulation of oleoresins from rosehip fruits for getting powders with multiple applications

Liliana Mihalcea [a], Bogdan Păcularu-Burada [a], Ștefania-Adelina Milea [a], Iuliana Aprodu [a], Nina-Nicoleta Condurache (Lazăr) [a], Elena Iulia Cucolea [b], George-Mădălin Dănilă [b], Adrian Cîrciumaru [c], Stănciuc Nicoleta [a,*]

[a] Dunărea de Jos University of Galati, Faculty of Food Science and Engineering, Domnească Street 111, 800201, Galati, Romania
[b] Cromatec Plus SRL, Research Center for Instrumental Analysis SCIENT, Petre Ispirescu Street 1, Tâncăbești, Ilfov, 077176, Romania
[c] Dunărea de Jos University of Galati, Cross-Border Faculty, Domnească Street 111, 800201, Galati, Romania

ARTICLE INFO

ABSTRACT

The supercritical fluids extraction (SFE) was used to extract the oleoresins from rosehip, followed by an in-depth phytochemical analysis and the development of two design-customized powders for different food and pharmaceutical applications. The SFE experiments allowed obtaining an oleoresins extraction yield of 11.85%. Two fractions were separated (S40 and S45), with significantly different phytochemical profile (p < 0.05), highlighting the efficiency of extraction of fatty acids in S40 extract, whereas the extraction of polyphenols, phytosterols, carotenoids and polyphenols was favored in S45 extract. The phytochemical profile revealed that the linoleic acid (C18:2) and α-linolenic acid (C18:3) represented approximatively 82% and 58% from the total fatty acid content in S40 and S45, respectively. α-Tocopherol and γ-tocopherol prevailed in both extract fractions, with a higher concentration in S45 (229.66 mg/g dry matter (DM) and 112.36 mg/g DM, respectively), whereas β-sitosterol was the major phytosterol in S45 fraction (118.75 mg/g DM). The S40 fraction was used to design two microencapsulated powders, by combining emulsification, complex coarcevation and freeze-drying. In order to develop new wall materials, with unique properties, the soy protein isolates were used for cross-linked reactions, by using an approach in one step (transglutaminase mediated) (coded as N) and two-steps (heat-induced and transglutaminase mediated) (coded as T). The N powder showed a better phytochemical content, leading to a higher antioxidant activity (5.27 mM Trolox equivalents/g DM), whereas for variant T, the bioactive were apparently doubled encapsulated.

1. Introduction

The current forecasts concerning the global population increase have a concomitant impact on the demand for production of enough food in order to fulfill the need for adequate and healthier nutrition, whereas turning the existing production and consumption systems into sustainable food alternatives (Koch et al., 2021). Therefore, both academia and industry intensified the efforts to identify new and alternative sources for food, meeting the abovementioned requirements.

Rosehips (*Rosa canina*), belonging to the Rosaceae family, is a well-known reddish-color fruit growing in Central Asian and Anatolian territories (Duru et al., 2011). The fruits have a short harvesting season and can be consumed as fresh or in processed forms (Erenturk et al., 2010). However, due to its slightly tart taste of the fresh fruit, the rosehips are consumed mainly as tea, jam, nectar, marmalade, and pestil (İlyaso-ğlu, 2014). The rosehip fruits' valorization is based on their rich content in phenolic compounds, carotenoids, tocopherols, C, A, B1, B2 and K vitamins, calcium, phosphorus, potassium minerals, carbohydrates (pectin), and essential oils (Medveckienė et al., 2020). Due to the complex phytochemical profile and biological activities, the rosehip fruits have been traditionally used as immunosuppressive, antioxidant, anti-inflammatory, anti-arthritic, analgesic, anti-diabetic, cardioprotective, antimicrobial, gastroprotective, and for skin ameliorative effects (Goztepe et al., 2022). Additionally, the rosehip seeds contain about 10% (*w/w*) oil, consisting mainly of linoleic (40.5%) and oleic acids (16%) (de Santana et al., 2016), with a significant concentration of trans-retinoic acid, known for its regenerative properties. Rosehip oil is commonly used in cosmetic and medical practices and products, mainly

for skin regeneration after scars (Franco et al., 2007). The fruits have been used in folk medicine for a long time due to their unique prophylactic and therapeutic properties against several diseases, such as colds, infectious diseases, gastrointestinal disorders, urinary tract diseases, and inflammatory diseases (Ouerghemmi et al., 2016). Although, rosehip fruits are potential sources of high-value compounds, the fruits are still not exploited at an industrial scale. To our knowledge, at the present time, there is no food chain for the valorization of rosehip fruits; in most cases, the production of these products is generally local (Özdemir et al., 2022). The industrial processing of these valuable compounds requests the application of appropriate techniques aiming for their efficient extraction, considering both the quality of the extracts and environmental impact. In this regard, green extraction techniques should be considered, such as the use of environmentally friendly, non-toxic, and tunable solvents, which could meet the technological and economic demands of the individual process (Vidovic et al., 2021). Supercritical carbon dioxide extraction (SFE) is generally recognized as an efficient alternative to the conventional liquid-solid extraction techniques, considered as time and energy-consuming. Additionally, SFE provides high affinity for lipophilic compounds and protective effect on oxidative and thermal damages. SFE allow to obtain high quality oils without further refining and no contamination of residual solid matrices. At industrial scale, SFE has become more relevant for the extraction of different types of matrices to obtain lipids and other bioactive for food, pharmaceutical, cosmeceutical and nutraceutical applications. However, when extracted from different matrices, the oleoresins are prone to oxidative and polymeric changes of the fat component and mono-terpene hydrocarbons, due to their highly sensitive behavior to environmental factors such as: humidity, heat, and oxygen. To limit these shortcomings, the application of microencapsulation techniques is required in order to protect the bioactive from external factors, improve the handling as pharmaceutical and food ingredients, and allow controlled release at specific target sites.

The use of encapsulating methods based on the cross-linking procedure has become increasingly popular in recent years. In general, a cross-link is defined as an interaction between molecules. Two types of cross-linking are known: chemical and physical. In the chemical cross-linking reaction, the polymer chains interact and form permanent junctions through the action of various agents. Considering the physical crosslinking, the polymer chains interact physically and chemically to form chemical bonds at weak junctions (Batista et al., 2019). A wide range of environmental factors (such as pH, temperature, or ionic strength) and physicochemical processes (such as hydrophobic interactions, charge condensation, hydrogen bonding, stereo-complexation, or supramolecular chemistry) can cause the physical crosslinking of polymer chains (Hoare and Kohane, 2008). Chemical cross-linking involves the use of a variety of substances, including natural (enzymes, genipin, vanillin, tannic acid, etc.) and synthetic cross-linkers (glutaraldehyde, carbodiimide, polycarboxylic acids, etc) (Alavarse et al., 2022).

The selection of soy protein isolates as wall-forming materials in microencapsulation align with the current "green" trend in the food, pharmaceutical and cosmetics industries (Li et al., 2012). When considering the use of plant-based proteins in different food applications, the allergenic potential should be considered, which is considerably lower compared to animal derived proteins. As wall materials, soy proteins are suitable for microencapsulation, due to their solubility, water and fat absorption, emulsion stabilization, gelation, foaming, plus good film-forming and organoleptic properties (Nesterenko et al., 2013).

The aims of this study were to obtain oleoresins from rosehip fruits by using SFE, whereas advanced profiling of the obtained extracts assumed the use of chromatographic methods for identification and quantification of fatty acids, tocopherols, phytosterols, carotenoids, and polyphenolic compounds. The selected extract was used to obtain microparticles, by combining emulsion, complex coacervation and freeze-drying using two cross-linked modified matrices. The one step cross-

linking reaction used was mediated by transglutaminase (sample coded as N), whereas the heat-induced and transglutaminase mediated cross-linked reaction of soy protein isolates were analyzed as a two steps customized design for rosehip oleoresins microencapsulation (sample coded as T). The impact of the thermal treatment on the particularities of main soy proteins and on the exposure of residues potentially involved in the transglutaminase assisted cross-linking reactions, was in-depth investigated by means of molecular modelling approach. The resulting powders were analyzed for the microencapsulation efficiency, advanced phytochemical profile, structure and morphology, and antioxidant activity.

2. Materials and methods

2.1. Fruits

Rosehip fruits (*Rosa canina* L.) were obtained from the local producer (Galați, Romania), harvested in the winter of 2021, at full maturity. The fruits were sorted, washed, crushed, immediately frozen ($-18\ ^\circ$C), and subjected to freeze-drying (CHRIST Alpha 1–4 LD plus, Germany) at $-42\ ^\circ$C under a pressure of 10 MPa for 48 h. The resulting powder with the diameter of the particle sizes passed through a stainless-steel mesh sieve between 0.2 and 0.4 mm was collected in dark glass containers and stored at 4 $^\circ$C until extraction. The rosehip powder oil content and the moisture content were $2.67 \pm 0.03\%$ (AOAC, 1998) and $5.42 \pm 0.01\%$, respectively.

2.2. Reagents and standards

Acetonitrile, formic acid, ethyl acetate, hexane, acetone, ethanol, methanol, β-cryptoxanthin, α-carotene, β-carotene, lycopene, gallic acid, caffeic acid, chlorogenic acid, p-coumaric acid, (+) - catechin, quercetin, kaempferol (HPLC-grade) and KOH (ACS reagent) were purchased from Sigma-Aldrich (Germany). All other reagents and solvents were of analytical and HPLC grade.

2.3. SFE of oleoresins from freeze-dried rosehip fruits

Extraction of oleoresins from freeze-dried rosehip fruits, including seeds was performed in a supercritical CO_2 pilot plant system (Natex, Prozesstechnologie GmbH, Austria, Fabr. no. 10–023/2011), operated continuously for fluid phase, with a batch for solid phase (0.405 kg/batch). The remaining volume of the extractor was filled with glass beads in the bottom and top of the cell. The system includes a chiller (Cooling Unit no.11030258, Hyfra-Industriekühlanlagen GmbH, Krunkel, Germany), an extractor with a volume of 2 L and two separators with volume 1.5 L (316-stainless steel), pressure regulators, thermometers and manometers automatically controlled by ABB software (ABB -Mannheim, Germany) and filters. The liquid CO_2 (purity 99.9%, Messer Romania Gaz S.R.L, Bucharest, Romania) was taken from the CO_2 tampon tank towards the pre-cooler at the temperature of $-3.5\ ^\circ$C and loaded to the extractor with a pressurization pump for CO_2 (LDE-M-2XXV1, serial no. 533822–010, Lewa Pumpen GmbH, Wien, Austria). The pressurized CO_2 was brought to the desired extraction and separation temperatures by means of heat exchangers on pipelines. Due to the fact that high extraction yield does not always contain high fatty acids (Machmudah et al., 2007), the SFE batches were carried out according to Jahongir et al. (2019) and Salgın et al. (2016), with some modification. The SFE parameters (pressure/temperature) for rosehip oleoresins were as follows: 35 MPa/45 $^\circ$C for extraction, 10 MPa/45 $^\circ$C for first separator (S40 fraction), while in the second separator (S45 fraction) the decompression up to a recirculation pressure 5 MPa and temperature 21 $^\circ$C were set. The extraction batches were carried out in the presence of the co-solvent, 5% of 96% ethanol (*v/w*) (Salgın et al., 2016) with the supercritical CO_2 mass flow rate of 0.42 kg/min. After 120 min of extraction (Jahongir et al., 2019), the resulting extracts were collected

and weighed immediately. By selecting these parameters, a minimal degradation of the bioactive during SFE was considered, compared to similar protocols (Machmudah et al., 2008). The extraction yield (%) was calculated by dividing the total amount of extract to the amount of initial extraction material.

2.4. Chromatographic analysis of carotenoids and polyphenolic compounds in the extracts

The carotenoids from the SFE extracted fractions were subjected to saponification prior to the HPLC analysis. Firstly, a sample aliquot was extracted for 2 h at 25 °C and 200 rpm (Lab Companion SI-300, GMI, Minneapolis, USA) in a solvent mixture of hexane, acetone, and ethanol (70:15:15 v/v/v). Then, saponification was made with KOH (40% w/v) solution in methanol for 2 h at 25 °C and 200 rpm (Can-Cauich et al., 2019). Finally, the supernatant obtained after centrifugation at 8000 rpm, 4 °C for 30 min (Hettich Universal 320R, Tuttlingen, Germany) was collected and used for the carotenoids analysis by HPLC. The carotenoids' separation by HPLC was assessed as Mihalcea et al. (2021) described at 450 nm. A C18 column (LiChrosorb PR-18, 125 × 4 mm, 5 μm particle size) was connected to the Agilent 1200 HPLC system equipped with an autosampler, degasser, quaternary pump system, multi-wavelength detector (MWD), and column thermostat (Agilent Technologies, Santa Clara, CA, USA). The separation and identification of the flavonoids and polyphenolic compounds from the rosehip extract were carried out by the same Agilent 1200 HPLC system using a Synergi Max-RP-80 Å column (250 × 4.6 mm, 4 μm particle size, Phenomenex, Torrance, CA, USA). The gradient elution system for the separation of the flavonoids and polyphenolic compounds was made of solvent A (ultrapure water: acetonitrile: formic acid = 87:3:10) and solvent B (ultrapure water: acetonitrile: formic acid = 40:50:10) as Antoniolli et al. (2015) described, with minor modifications. A gradient separation by the following pattern was used: 0 min–94% A; 20 min–80% A; 35 min–60% A, 40 min–40% A, 45 min–10% A. The method runtime was 80 min, with the optimal flow rate of 0.50 mL/min at 30 °C and an injection volume of 20 μL. The compounds of interest were identified at 280 nm and 320 nm. The identification of the carotenoids, flavonoids, and polyphenolic compounds from the rosehip extract was made by comparing the retention times of the unknown peaks with the retention times obtained for standard solutions of bioactives. Thereafter, the identified compounds were quantified by external calibration curves using the peak area. Data acquisition was made by Chemstation software, version B.04.03 (Agilent Technologies, Santa Clara, CA, USA). Results were expressed in mg/100 g DW raw material.

2.5. Microencapsulation of rosehip oleoresins

In order to obtain rosehip fruits oleoresin microparticles, the matrices for microencapsulation were obtained by cross-linking reactions using soy protein isolates, in one (sample coded N) and two steps (sample coded T). A stock protein solution (100 mL of 50 mg/mL) was prepared by hydration in ultrapure water. Protein solution was homogenized at 450 rpm and 30 °C for 2 h using a magnetic stirrer (IKA RCT Basic, Staufen Germany). For the double cross-linking, a volume of 50 mL was thermally treated on a water bath at 85 °C for 20 min, and then was cooled on ice. Next, both protein solutions, with and without thermal treatment, were stored at 4 °C for 24 h. Subsequent, transglutaminase was added in both protein solutions in a 4:1000 enzyme/substrate ratio, and the cross-linking process took place for 8h at 50 °C on a heating magnetic stirrer. To inactivate the enzyme, both solutions were thermally treated at 85 °C for 5 min on a water bath, followed by cooling on ice. Next, 2% of S40 fraction of rosehip extract was added to both protein solutions, homogenized for 1h at 450 rpm at room temperature, and then the pH was lowered to 4.0. Afterward, the mixtures were frozen overnight. Stabilization of the microcapsules was achieved by freeze-drying using an Alpha 1–4 LD plus equipment (CHRIST,

Osterode am Harz, Germany) for 72 h, at −42 °C under a pressure of 10 MPa. The powders were collected in glass containers and hermetically sealed and stored at 4 °C until analysis.

2.6. In silico analysis

In order to highlight the impact of the thermal treatment applied to the soy proteins prior to cross-linking reactions, single molecule level investigations were carried out using the molecular modelling approach. The models of the main soy proteins, namely α' homotrimer of β-conglycinin (1UIKpdb; Maruyama et al., 2004) and of the homotrimer of A1aB1b subunits (1FXZ.pdb; Adachi et al., 2001), were selected from the RCSB Protein Data Bank. These single molecule models were further called 7S and 11S, respectively. The molecular models were subjected to refinement, optimization *in vacuum*, solvation using explicit water molecules and energy minimization of the solvated complexes, such as to be prepared for further molecular dynamics simulations. In agreement with the conditions employed in the laboratory scale experiment, the solvated protein models were heated and finally equilibrated at 50 °C and 85 °C. All molecular mechanics and molecular dynamics steps were carried out using the Gromacs 5.1.1 package (Abraham et al., 2015), as reported by Dumitrașcu et al. (2020). Energy and structural details regarding the final soy proteins models were collected using the dedicated tools of Gromacs software.

2.7. Microencapsulation efficiency

The powders were evaluated regarding the total carotenoid content and encapsulation efficiency, using the method described by Mihalcea et al. (2018) that quantifies the total (TC) and surface carotenoids (SC). Regarding the TC, 200 mg of each powder were solubilized in 6 mL of 10% NaCl and methanol mixture (1:1 ratio). After 30 min of rest, 30 mL of *n*-hexane and acetone (3:1) were added. The mixtures were sonicated for 30 min at 25 °C (40 kHz) and centrifuged at 14000 rpm for 10 min at 4 °C. TC were quantified by reading the absorbance of 3 mL from each supernatant at 470 nm (Biochrom, Cambridge, UK). The SC was quantified by dissolving 20 mg of each powder in 10 mL of *n*-hexane and acetone (1:1 ratio), followed by 2 min of vortexing. Then, the samples were centrifuged at 14000 rpm for 10 min at 4 °C. SC was quantified by reading the absorbance of 3 mL from each supernatant at the same wavelength mentioned above. The encapsulation efficiency (EE) was calculated using the equation (1):

$$EE\ (\%) = \frac{TC - SC}{TC} \times 100 \tag{1}$$

Total flavonoid (TFC) and polyphenol contents (TPC) were also assessed. For this purpose, 200 mg of each powder were solubilized in 70% aqueous ethanol and sonicated for 30 min at 25 °C and 40 kHz. Then, the mixtures were centrifuged at 14000 rpm for 10 min at 4 °C. The supernatant was used for TFC and TPC quantification as described hereunder.

2.8. Global phytochemicals profiling of free and microencapsulated oleoresins

Both free and microencapsulated oleoresins were characterized by quantifying the lipophilic and hydrophilic compounds using spectrophotometric methods. In case of the microencapsulated oleoresins, the supernatants obtained from microencapsulation efficiency for TC evaluations were used for analysis.

For the evaluation of lipophilic compounds concentrations, 100 mg of each extract were dissolved in 5 mL of *n*-hexane and acetone (3:1 ratio), whereas for quantifying the hydrophilic compounds, 100 mg of each extract were dissolved in 5 mL of 70% aqueous ethanol. Both mixtures were vortexed for 1 min and then sonicated at 40 kHz for 30 min at 25 °C. Next, the mixtures were centrifuged at 14000 rpm for 10

min at 4 °C. The resulted supernatants were analyzed in terms of β-carotene (BC), lycopene (LC), TFC, and TPC. BC and LC contents were determined by reading the absorbance of 3 mL from the lipophilic supernatant at 470 nm and 503 nm, respectively, using a Libra S22 UV–VIS spectrophotometer (Biochrom, Cambridge, UK). The concentrations of lipophilic compounds were calculated using the equation (2) (Neagu et al., 2020):

$$\text{Concentration of lipophilic compounds (mg / g)}: \frac{\text{Abs} \times \text{Mw} \times \text{Df}}{\epsilon \times \text{L} \times \text{m}} \quad (2)$$

where: Abs - absorbance at 503 nm and 470 nm, respectively, Mw - molecular weight for lycopene (536.873 g/Mol) and β-carotene (536.8726 g/Mol), Df - sample dilution rate, ε-molar absorptivity for lycopene (3450 L/Mol·cm) and β-carotene in *n*-hexane and (2500 L/Mol·cm), L-cell diameter of the spectrophotometer (1 cm), and m – mass of the extracts.

In order to determine TFC, the aluminum chloride (AlCl₃) based spectrophotometric method was applied. In brief, 0.25 mL of each hydrophilic supernatant were mixed with 2 mL of distilled water and 0.075 μL of 5% NaNO₂ solution and allowed to rest for 5 min. Next, 0.15 mL of 10% AlCl₃ solution were added and left to rest for another 6 min. Subsequently, 0.5 mL of 1 M NaOH solution was added, and the absorbance of the mixtures was immediately measured at 510 nm (Roman et al., 2021). Results were expressed as mg catechin equivalents (CE)/g dry matter (DM), using a calibration curve.

Folin-Ciocâlteu colorimetric method was applied to quantify the TPC of the extracts. Briefly, 0.20 mL of each hydrophilic supernatant were mixed with 15.8 mL of distilled water and 1 mL of Folin–Ciocâlteu reagent. Further, the mixtures were allowed to rest for 10 min, and then 3 mL of 20% Na₂CO₃ solution were added. Afterward, the mixtures were kept at dark at room temperature, and after 60 min, the absorbance of the mixtures was measured at 765 nm (Roman et al., 2021). Results were expressed as mg gallic acid equivalents (GAE)/g DM, using a calibration curve.

2.9. Fatty acids

Fatty acids from free and microencapsulated SFE oleoresins were first converted into methyl esters (FAMEs) using the methanolic boron trifluoride (BF3)-catalyzed esterification procedure, as described by Mihalcea et al. (2021). In brief, 100 ± 5 mg of material were weighted in a 50 mL round bottom flask, followed by addition of 4 mL of 0.5 M methanolic NaOH and the mixture was refluxed for 30 min. A volume of 5 mL of 15% (v/v) methanolic BF3 was then added in the flask and refluxed for another 3–5 min. After cooling, the organic fraction containing FAMEs was extracted 3 times with 3 mL of *n*-hexane, followed by dilution to 20 mL with *n*-hexane. A volume of 1 μL of FAMEs extract was injected into the gas-chromatographic system coupled with a mass spectrometer (Perkin Elmer Clarus 680/SQ 8T, Perkin Elmer, CT, USA) equipped with an Elite-WAX capillary column (30 m × 0.25 mm i.d., 0.25 μm film thickness (Perkin Elmer, CT, USA), using helium as carrier gas (flow rate of 1.5 mL/min). Mihalcea et al. (2021) described the operational conditions for fatty acids identification and quantifications. The quantification of FAMEs present in the material was performed in selected ion recording mode (SIR), using a 5-points calibration curve prepared from 37 component FAME Mix (Supelco, Sigma-Aldrich, Darmstadt, Germany). The experiments were performed in duplicate.

2.10. Phytosterols and tocopherols

The free and microencapsulated oleoresins dissolved in *n*-hexane were used to analyze the phytosterols profile via GC-MS. The working volume of 2 mL of dissolved material was evaporated to dryness under nitrogen-free oxygen stream. Then, the residues were derivatized using 100 μL of MSTFA (Mackerey-Nagel, Dueren, Germany) at 60 °C and for 45 min. A volume of 1 μL was injected in the GC-MS system equipped with an Elite-5ms capillary column (30 m × 0.25 mm i.d., 0.25 μm film thickness of 5% phenyl-95% methylpolysiloxane, Perkin Elmer, CT, USA), using helium as carrier gas (flow rate 1.0 mL/min). Mihalcea et al. (2021) described the operational conditions for phytosterols and tocopherols identification and quantifications. The identification was achieved in the full scan mode with scanned mass range 100–600.

2.11. Antiradical scavenging activity

In order to assess the radical scavenging ability of the free and microencapsulated rosehip fruits SFE oleoresins, the Trolox Equivalent Antioxidant Capacity (TEAC) method was performed by using the 2,2-azinobis-3-ethyl-benzothialzoline-6-sulfonic acid (ABTS•+) radical cation decoloring reaction. In brief, the ABTS + stock solution was prepared at a concentration of 2.45 mM final concentration, by mixing the ABTS•+ aqueous solution with a potassium persulfate solution (7.0 mM). The ABTS + stock solution was allowed to react for 16 h in the dark at room temperature. For evaluation of TEAC, a volume of 0.05 mL of oleoresin extracts was added to a volume of 1.95 mL of the ABTS•+ solution and allowed to react for 2 h in the dark. The absorbance of the mixture was measured at 734 nm (Libra S22, Biochrom, Cambridge, UK). The antioxidant activity was expressed as mM TEAC/g dw, based on the calibration curve.

2.12. Statistical analysis

The statistical analysis of the data was carried out using the Minitab 17 software. By using the One-way Anova method and Tukey test, the differences between the samples were evidenced. All experiments were done in triplicates, and the results were expressed as average values with a standard deviation. For the HPLC analysis of the polyphenols and carotenoids, results were assessed from two independent supercritical extracts.

3. Results and discussion

3.1. SFE oleoresins extraction yield and global phytochemical profile of the extracts

Due to the fact that the extraction parameters were adjusted to allow the extraction of bioactive enriched oleoresins, the co-solvent assisted SFE from freeze-dried rosehip fruits was performed at 35 MPa and 45 °C, for 120 min. The selected parameters allowed to obtain an extraction yield of 11.85%. Salgın et al. (2016) reported higher extraction yield (15.6 g oil/100 g dry solid) at 30 MPa and 40 °C, for an extended extraction time of 5 h. The lower extraction yield reported in this study could be explained by the competition between solvent density and solute vapor pressure (Machmudah et al., 2007) at higher pressure. Therefore, the higher pressure used in this study (35 MPa) allowed to obtained two fractions enriched in fatty acids. Both SFE fractions were characterized by quantifying the lipophilic and hydrophilic compounds (Table 1). The resulting SFE fractions showed a significantly different (p < 0.05) phytochemical profile. Regarding the lipophilic compounds, S40 fraction contains an almost double concentration of BC and LC compared to the S45 fraction (Table 1). Concerning the hydrophilic compounds, S40 fraction showed a significantly higher concentration of TPC than S45 (p < 0.05). However, when considering TFC and antioxidant activity, no significant differences between the two fractions (p > 0.05) were found. Therefore, a high correlation between the total phenolic content and the antioxidant activity of rosehip extracts may be suggested, as reported by Taneva et al. (2016). These authors highlighted that the 50% ethanol extracts of rosehip fruits showed a content of polyphenols of 6.9 g GAE/100 g and an antioxidant activity, based on DPPH assay, of 368.4 TEAC/g DM. It has been reported that the main carotenoids in rosehip fruits are LC and BC, both of which are

Table 1

Advanced phytochemical profile of CO_2 rosehip fractions after supercritical extraction.

Bioactives	Fractions	
	S40	S45
Global characterization (/g DM)		
β-carotene (mg)	522.06 ± 3.77[a]	293.22 ± 6.60[b]
Lycopene (mg)	214.98 ± 5.36[a]	100.43 ± 2.90[b]
Total flavonoid content (mg CE)	1.11 ± 0.02[a]	0.94 ± 0.09[b]
Total polyphenol content (mg GAE)	2.65 ± 0.07[a]	2.28 ± 0.05[b]
Antioxidant activity (mM TEAC)	12.80 ± 0.48[a]	13.13 ± 0.48[a]
Polyphenols (mg/100 g DM)		
(+) - Catechin	101.66 ± 0.00[b]	167.67 ± 1.15[a]
Chlorogenic acid	15.75 ± 1.33	Nd
Caffeic acid	8.55 ± 0.27	Nd
p-Coumaric acid	13.17 ± 0.15	Nd
Quercetin	14.57 ± 0.48	Nd
Kaempferol	16.78 ± 0.15	Nd
Gallic acid	Nd	83.16 ± 0.28
Fatty acids (mg/g DM)		
Myristic acid (C14:0)	2.02 ± 0.12[a]	1.99 ± 0.017[a]
Pentadecanoic acid (C15:0)	0.92 ± 0.029[a]	0.92 ± 0.002[a]
Palmitic acid (C16:0)	25.84 ± 4.74[b]	33.72 ± 0.81[a]
Palmitoleic acid (C16:1)	1.80 ± 0.04[b]	2.06 ± 0.04[a]
Stearic acid (C18:0)	12.31 ± 1.91[a]	13.90 ± 0.33[a]
Oleic acid (C18:1)	46.54 ± 1.57[a]	48.15 ± 1.68[a]
Linoleic acid (C18:2)	287.95 ± 14.79[a]	295.45 ± 9.12[a]
α-Linolenic acid (C18:3)	119.00 ± 12.06[a]	1.99 ± 0.02[b]
Total fatty acids	**496.39 ± 9.86**	**398.18 ± 16.97**
Tocopherols (mg/g DM)		
α-tocopherol	89.52 ± 3.44[b]	229.66 ± 6.79[a]
γ-tocopherol	37.85 ± 1.02[b]	112.36 ± 3.47[a]
σ-tocopherol	0.89 ± 0.09[b]	3.25 ± 0.56[a]
β-tocopherol	0.97 ± 0.78[b]	2.88 ± 0.88[a]
Total tocopherols	**129.23 ± 7.53**	**348.15 ± 16.54**
Phytosterols (mg/g DM)		
β-sitosterol	63.36 ± 1.02[b]	118.75 ± 1.76[a]
Campesterol	2.55 ± 0.99[b]	5.05 ± 1.01[a]
α-Amyrin	1.13 ± 0.02[b]	2.55 ± 0.89[a]
β-amyrin	0.45 ± 0.12[a]	0.44 ± 0.12[a]
Total physterols	**67.49 ± 4.45**	**126.79 ± 5.34**
Carotenoids (mg/g DM)		
β-cryptoxanthin	149.14 ± 2.73	Nd
β-carotene	63.46 ± 5.31	Nd
α-carotene	5.23 ± 0.35[b]	7.91 ± 0.21[a]
Lycopene	Nd	0.54 ± 0.09

Values from a line that share same superscript letter (a, b) are not significantly different (p > 0.05). Measurements are expressed as mean ± SD of triplicate. For the HPLC data, the values are given as average for duplicate measurements (n = 2) ± standard deviations; Nd – not determined.

hydrophobic and may be dissolved in non-polar chemical solvents such as tetrahydrofuran, hexane, chloroform, and acetone but are basically insoluble in polar solvents such as water and ethanol (Horvath et al., 2012). Sernaite et al. (2019) used SFE to isolate lipophilic components from rosehip extracts and a maximum yield was obtained at temperature of 75.2 °C, pressure of 44 MPa and time of 115 min, which allowed the recovery of 65% of the extractable lipophilic compounds. SFE was developed in response to the demand for safer techniques of extracting carotenoids in lipophilic extracts (extracted from natural plant sources) (Zuknik et al., 2012).

3.2. Advanced phytochemical profile of rosehip oleoresins fractions

The HPLC analysis of the SFE rosehip oleoresins allowed to separate 11 carotenoids from the fraction S40 (Fig. 1, a), with β-cryptoxanthin as the major compound (149.14 mg/g DM), followed by BC (63.46 mg/g DM), and α-carotene (5.23 mg/g DM). On the opposite, the fraction S45 was characterized by an increased concentration of α-carotene (7.91 mg/g DM) and LC (0.54 mg/g DM) (Fig. 1, b).

(a)

(b)
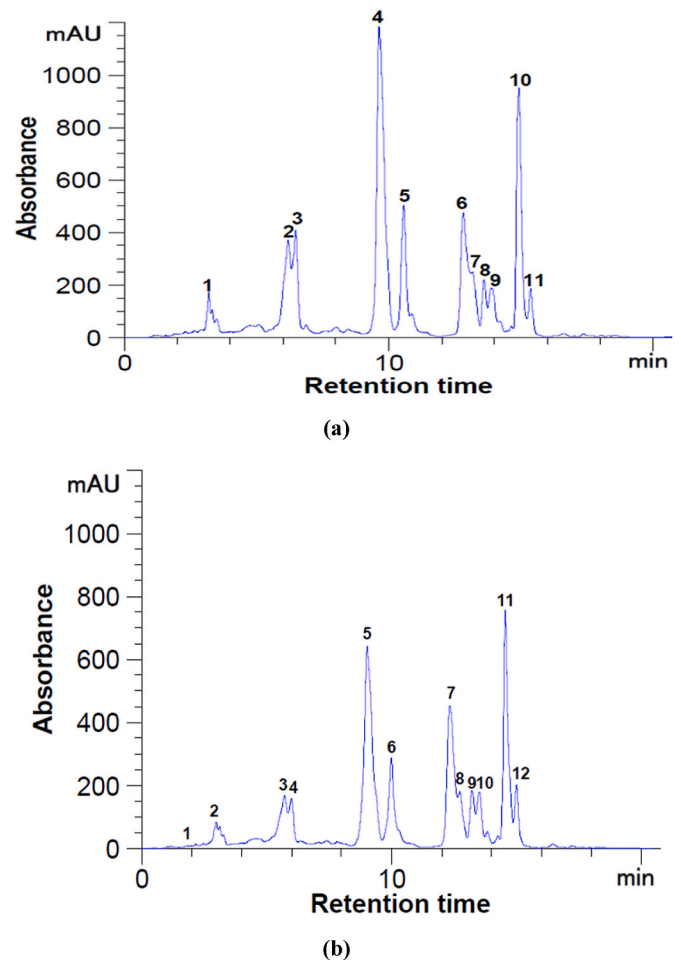
Fig. 1. HPLC chromatograms for the carotenoids from rosehip extract at 450 nm within the fractions S40 (a) and S45 (b). Peaks' identification: (a): 4 – β-cryptoxanthin; 8 – α-carotene; 11 – β-carotene 1–3, 5–7, 9, 10 – unidentified peaks; (b): 1 – lycopene; 10 – α-carotene; 2–9, 11, 12 – unidentified peaks.

The flavonoids and polyphenols content in the SFE rosehip oleoresins, respectively fraction S40 and S45 are shown in Table 1. An enriched polyphenolic profile can be observed in the fraction S40, comprising phenolic acids (caffeic, *p*-coumaric, chlorogenic) with concentrations ranging between 8.55 and 15.75 mg/100 g DM. Kaempferol (16.79 mg/100 g DM) and quercetin (14.57 mg/100 g DM) were also identified. Hence, gallic acid was identified only in the S45 fraction, whereas (+)-catechin was the major flavonoid within both S40 and S45 fractions, with a slightly increased concentration in the S45 fraction (Table 1). Our experimental results are in good agreement with other studies. However, it should be mentioned that bioactives' profile highly depends on the preliminary preservation techniques applied to the raw rosehip fruits. Compared to our experimental data, higher concentrations of catechin, quercetin, kaempferol, p-coumaric, and gallic acid were determined by analyzing the methanolic extracts of rosehip fruits subjected to different drying methods (Goztepe et al., 2022). Moreover, such differences regarding the polyphenolic profile could be attributed to the geographical area, environmental factors, rosehip fruits' harvesting time or CO_2 and HPLC separation methods. In processed products, catechin was the main bioactive compound within the rosehip-based beverages, whereas lower concentrations of gallic acid and quercetin were associated with the rosehip juice, wine, or vinegar (Özdemir et al., 2022).

The fatty acids profile of the oleoresins fraction is shown in Table 1. In fraction S40, the global fatty acids concentration was 496.39 mg/g DM, whereas a lower concentration was found in the S45 fraction, of

398.18 mg/g DM. The linoleic acid was predominant in both fractions, with concentrations of 287.95 mg/g DM and 295.45 mg/g DM, respectively, representing approximately 58% of the total fatty acids. The α-linolenic acid (C18:3) was the second polyunsaturated fatty acid found in fraction S40 (119.00 mg/g DM) and oleic acid in S45 (48.15 mg/g DM) (Table 1).

Four phytosterols were found in rosehip oleoresin fractions, such as β-sitosterol, campesterol, α- and β-amyrin. The predominant phytosterol in both fractions was β-sitosterol (63.36 mg/g DM in S40 and 118.75 mg/g DM in S45, respectively), followed by campesterol (2.55 mg/g DM and 5.05 mg/g DM, respectively). For β-sitosterol, campesterol, and α-amyrin, an increased concentration in S45 can be observed, whereas for β-amyrin no significant differences between the two fractions were found (Table 1).

The tocopherols profile of oleoresin fractions is shown in Table 1. Four tocopherols were identified: α-tocopherol as predominant (69% in S40 and 66% in S45), followed by γ-tocopherol, σ-tocopherol, and β-tocopherol. The total tocopherols content in S40 was 129.23 mg/g DM, whereas in S45 a three-fold higher concentration was separated (348.14 mg/g DM).

3.3. Phytochemical profile of microencapsulated oleoresins from rosehip fruits

Two powders were obtained through microencapsulation of rosehip oleoresins from the S40 fraction, using one (N) and double (T) cross-linked soy proteins isolates. Table 2 presents the results of the phytochemical characterization of the two powders. When compare the polyunsaturated fatty acid profile of the two powders with the extract, it can be observed that both variants allowed a concentration of the myristic, pentadecanoic, palmitic, palmitoleic and stearic acids, whereas a lower content in oleic, linoleic and α-linolenic acids was found. It has been found that, compared to simple cross-linked soy proteins (N), the double cross-linked ones (T) retained a significantly lower concentration of biologically active compounds ($p < 0.05$). Thus, it can be observed that the N powder had the maximum encapsulation efficiency of total carotenoids of 51.55%, whereas a lower value of 42.40% was observed for powder T. The concentrations of encapsulated BC, LC, and TFC showed the same pattern. Thus, the powders contained a BC content of 162.30 mg/g DM in powder coded N, and 137.54 mg/g DM in powder T. The N variant showed a significant higher LC content of 64.35 mg/g DM ($p < 0.05$). No significant differences were found in TFC (1.95 mg CE/g DM and 1.61 mg CE/g DM in N and T, respectively) and in TPC (5.12 mg GAE/g DM for N and 5.01 mg GAE/g DM in N and T, respectively).

The advanced phytochemical profiles of the powders, in terms of fatty acids, phytosterols and tocopherols are showed in Table 2. It can be observed that the single step cross-linking reaction allowed to obtain freeze-dried microencapsulated oleoresins with a higher global content in fatty acids, of approximatively 165 mg/g DW when compared with 117 mg/g DW in case of double step cross-linking reaction (sample T). From Table 2 it can be observed that higher amounts of individual fatty acids were found in sample N, highlighting a better microencapsulation efficiency for the most of the fatty acids, excepting the palmitoleic acid (C16:1). A global microencapsulation efficiency of approximately 67% and 71% for fatty acids was estimated for powder N and T, respectively. Comparing the fatty acid profile of the S40 fraction with the corresponding profile in the microencapsulated variants, it can be seen that the customized design used for the wall materials allowed retaining a significantly higher concentration of saturated fatty acids such as myristic, pentadecanoic, stearic and palmitic acids. The highest concentration of saturated fatty acids was observed for pentadecanoic and myristic acids in variant N. The concentration of omega-7 fatty acids increased significantly in both powders, from 1.80 mg/g in S40 to 14.64 mg/g and 16.14 mg/g in variant N and T, respectively. However, the techniques applied in our study allowed a significantly higher microencapsulation efficiency of saturated and omega-7 fatty acid when compared with monounsaturated omega-9 and the essential fatty acids. The powders retained only 9% and 5% of linoleic acid in variant N and 5% in variant T, respectively. A better retention was found for the α-linolenic acid, which represented approximately 16% in variant N and 9.5% in variant T.

The decreasing trend was observed for both powders, except for phytosterols. As regarding the phytosterols and tocopherols (Table 2), both powders preserved the four phytosterols profile of the extracts, with a predominance of β-sitosterol (88.04 mg/g DW in powder N and 29.55 mg/g DW in powder T), followed by α-amyrin, campesterol, and β-amyrin, respectively. However, when considering the total phytosterol content in the two powders, the N sample showed a content about 3 times higher compared to sample T. The one step transglutaminase mediated cross-linked allowed a significant increase in β-sitosterol, α- and β-amyrin, especially in variant N. All four tocopherols identified in the extracts were found in the freeze-dried samples, with a higher concentration of α-tocopherol in powder N (13.83 mg/g DM). The N sample showed a higher total tocopherols content (15.16 mg/g DW) when compared with T (2.35 mg/g DW).

In the attempt to gather details on the impact of thermal treatment on the availability of main soy proteins to act as substrate for transglutaminase cross linking, molecular modelling investigations were employed. The representative three-dimensional models of the glycinin and β-conglycinin fractions, representing nearly 40% and 30%, respectively of the total protein content of soybean (Maruyama et al., 2001), were equilibrated at temperatures of 50 °C and 85 °C (working on the assumption that all conformation changes of the proteins heated at higher temperature are irreversible), therefore resembling the conditions applied to obtain the N and T samples at laboratory scale. Regardless of the investigated protein model, important differences in terms of energy descriptors can be observed when comparing the results collected at different temperatures (Table 3). The higher total energy

Table 2
Advanced phytochemical profile of microencapsulated CO_2 rosehip oleoresins.

Compounds	N	T
Global characterization		
Total carotenoids encapsulation efficiency (%)	51.55 ± 1.56[a]	42.40 ± 3.01[b]
β-carotene (mg/g DM)	162.30 ± 4.22[a]	137.54 ± 6.97[b]
Lycopene content (mg/g DM)	64.35 ± 2.25[a]	55.64 ± 2.06[b]
Total flavonoid content (mg CE/g DM)	1.95 ± 0.07[a]	1.61 ± 0.10[b]
Total polyphenol content (mg GAE/DM)	5.12 ± 0.22[a]	5.01 ± 0.11[a]
Antioxidant activity (mM TEAC/g DM)	5.27 ± 0.04[a]	4.53 ± 0.08[b]
Fatty acids (mg/g DM)		
Myristic acid (C14:0)	16.85 ± 0.04[a]	11.35 ± 0.02[b]
Pentadecanoic acid (C15:0)	9.21 ± 0.01[a]	6.17 ± 0.01[b]
Palmitic acid (C16:0)	35.39 ± 0.73[a]	27.51 ± 0.36[b]
Palmitoleic acid (C16:1)	14.64 ± 0.28[b]	16.14 ± 0.21[a]
Stearic acid (C18:0)	21.79 ± 0.05[a]	14.39 ± 0.04[b]
Oleic acid (C18:1)	22.47 ± 0.29[a]	15.57 ± 0.05[b]
Linoleic acid (C18:2)	25.58 ± 0.69[a]	14.78 ± 0.28[b]
α-Linolenic acid (C18:3)	18.96 ± 0.63[a]	11.35 ± 0.01[b]
Total fatty acids	**164.90 ± 3.84**	**117.26 ± 1.38**
Tocopherols (mg/g DM)		
α-tocopherol	13.83 ± 0.87[a]	2.17 ± 0.29[b]
γ-tocopherol	0.80 ± 0.09[a]	0.16 ± 0.01[b]
σ-tocopherol	0.12 ± 0.01[a]	0.02 ± 0.01[b]
β-tocopherol	0.41 ± 0.02[a]	0.004 ± 0.001[b]
Total tocopherols	**15.16 ± 1.40**	**2.35 ± 0.43**
Phytosterols (mg/g DM)		
β-sitosterol	88.04 ± 1.17[a]	29.55 ± 2.05[b]
Campesterol	2.59 ± 0.56[a]	0.88 ± 0.01[b]
α-Amyrin	2.82 ± 0.44[a]	0.80 ± 0.07[b]
β-amyrin	0.66 ± 0.09[a]	0.26 ± 0.10[b]
Total physterols	**94.11 ± 3.19**	**31.49 ± 3.15**

Values from a line that share same superscript letter (a, b) are not significantly different ($p > 0.05$). Measurements are expressed as mean ± SD of triplicate. For the HPLC data, the values are given as average for duplicate measurements (n = 2) ± standard deviations; Nd – not determined.

Table 3

Single molecule level details on the effect of temperature on main soy proteins (7S and 11S).

Molecular descriptors	7S		11S	
	50 °C	85 °C	50 °C	85 °C
Energy descriptors				
Potential energy, kJ/mol	$(-2418.77 \pm 1.41) \cdot 10^{3\ b}$	$(-2286.04 \pm 1.54) \cdot 10^{3\ a}$	$(-2448.11 \pm 1.53) \cdot 10^{3\ b}$	$(-2314.16 \pm 1.46) \cdot 10^{3\ a}$
Total energy, kJ/mol	$(-1694.01 \pm 1.05) \cdot 10^{3\ b}$	$(-1483.00 \pm 1.06) \cdot 10^{3\ a}$	$(-1711.46 \pm 1.49) \cdot 10^{3\ b}$	$(-1497.73 \pm 0.95) \cdot 10^{3\ a}$
Surface descriptors				
Total surface exposed to solvent, nm^2				
protein	428.88 ± 3.79^a	422.02 ± 2.69^b	408.91 ± 2.35^a	395.92 ± 2.72^b
Gln residues	33.61 ± 1.09^a	33.34 ± 0.76^a	44.19 ± 0.86^a	36.84 ± 0.50^b
Lys residues	73.49 ± 1.39^a	73.12 ± 0.65^a	47.54 ± 0.68^a	47.81 ± 0.42^a
Hydrophobic surface exposed to solvent, nm^2				
protein	208.66 ± 2.34^a	202.03 ± 2.016^a	203.77 ± 1.39^a	198.10 ± 1.59^a
Gln residues	11.93 ± 0.38^a	11.33 ± 0.21^b	15.42 ± 0.42^a	13.06 ± 0.47^a
Lys residues	54.84 ± 0.95^a	54.08 ± 0.64^a	34.88 ± 0.54^a	35.29 ± 0.52^a
Hydrogen bonding				
Number of hydrogen bonds				
within protein	880 ± 14^a	838 ± 7^b	892 ± 14^a	871 ± 18^b
involving Gln residues	71 ± 5^a	76 ± 7^a	102 ± 6^b	117 ± 10^a
involving Lys residues	47 ± 6^a	43 ± 5^a	39 ± 4^b	36 ± 1^a
Number of hydrogen bonds between solute and water				
protein – water	1752 ± 27^a	1714 ± 28^b	1501 ± 26^a	1424 ± 23^b
Gln residues – water	119 ± 5^a	120 ± 5^a	166 ± 9^a	126 ± 7^b
Lys residues – water	188 ± 8^a	183 ± 7^a	137 ± 7^a	128 ± 6^b

For a soy protein (7S or 11S), values from a line that share same superscript letter (a, b) are not significantly different (p > 0.05).

values registered at 85 °C are a consequence of the increased thermal motion of the particles, compared to the corresponding system equilibrated at 50 °C. In the case of both investigated models a slight reduction of the total surface available to the solvent was noticed when increasing the temperature from 50 °C to 85 °C (Table 3). As a consequence of the rather good thermal stability of the proteins, the decrease of the total number of hydrogen bonds involved in stabilizing the protein structure was limited to ~5 and 2% in case of 7S and 11S, respectively.

Particular attention was paid to Gln and Lys residues from 7S to 11S structure, which are involved in the cross-linking reaction catalyzed by transglutaminase. Both proteins considered as models for the molecular modelling investigation are rich in Gln and Lys, which are rather well balanced. 7S has 60 Lys and 66 Gln residues, whereas 11S has 48 Lys and 78 Gln residues, all having good exposure to the solvent (Fig. 2), and therefore being available to be recognized by transglutaminase and to participate to the intra- and intermolecular cross-linking. No important differences in the Gln and Lys total and hydrophobic surface exposure to the solvent was noticed when subjecting the soy proteins to increasing temperature. The only exception concerns the 11S model, in which case the total Gln surface available to the solvent decrease by ~17%, while the Gln hydrophobic exposure decreased by 15% when raising the temperature from 50 °C to 85 °C (Table 3). Because of the local rearrangements within the conformation of the proteins, some changes in the contribution of the Gln and Lys residues to defining different types of well-ordered and stable secondary structure motifs were observed at

different temperatures. For instance, the temperature increase resulted in the 18% increase of the total number of Gln residues involved in hydrogen bonding network stabilizing the α-helices within 7S, whereas in case of 11S the participation of Gln to defining strands increased by 27%. These kind of atomic level changes targeting amino acids recognized by the enzyme, coupled with the more limited exposure of Gln at higher temperature might explain the lower ability of T sample to bind and encapsulate the biologically active compounds extracted from rosehip.

Rosehip prepared purees with encapsulating agents are an attractive food ingredient high in fiber and minerals that might be employed in the food industry to create various functional foods (Igual et al., 2022). Obtaining a powdered product would stimulate its consumption as a rehydrated juice or infusion, or to be added to sweets, dairy products, salads, ice cream, snacks, and even to enhance nearly any cuisine with bioactive elements (Igual et al., 2021). Comparing the encapsulating agents studied in the literature, the bioactive compound profiles behaved differently. In the case of carotenoids, the use of pea protein allowed obtaining a rosehip powder product with a higher content of carotenoids (45.9 ± 0.2 mg BC/100 g); however, the content of phenolic compounds was higher in the rosehip sample encapsulated with maltodextrin (1275.0 ± 4.0 mg GAE/100 g) (Igual et al., 2022). Concerning the cross-linked microencapsulation technique, Neagu et al. (2020) studied the oleoresin supercritical extracts from sea buckthorn encapsulated in whey proteins isolate and casein, in two states: native (N) and cross-linked mediated by transglutaminase (TG) and proved that cross-linked aggregates mediated by transglutaminase applied for microencapsulation of oleoresins have the potential to become new delivery systems for carotenoids and LC.

3.4. Antioxidant activity of the powders

In our study, the free radical scavenging capacity of the powders was tested on the ABTS radical (Table 2). As expected, N powder presented the highest antioxidant activity of 5.27 mM TEAC/g DW, compared to 4.53 mM TEAC/g DW for powder T. The high antioxidant activity of N powder could be correlated to the carotenoids and flavonoids content. Igual et al. (2022) obtained high values for antioxidant capacity, depending on the encapsulating material, ranging from 607.00 ± 13.00 mg TEAC/100 g to 955.00 ± 4.00 mg TEAC/100 g by DPPH method. This result indicates that rosehip can be used as a reliable source of natural antioxidants. The study of various *Rosa* species for antioxidant capabilities may raise awareness of their potential as a functional food or food additive.

3.5. Structure and morphological properties of the powders

The structure and morphological particularities of the powders are showed in Fig. 3. The appearance of the microparticles highlighting that the matrix structure of one-step cross-linked network (N sample) (Fig. 3, a) was not significantly different from the corresponding two-steps cross-linked one (T sample) (Fig. 3, b). In both freeze-dried samples, the oleoresins-loaded microparticles generally exhibited an amorphous-like structure, evidencing clusters of oils adhered and/or absorbed on the external surface of the biopolymeric microparticles. The obtained spherical microparticles are highlighted in Fig. 3a and b (at magnification of 20 000 ×) as structures, that are partially attached to the surface of the encapsulating matrix. However, the spherical formations fixed in the microencapsulation matrices were more abundant in N sample, which correlates with the microencapsulation efficiency values. Different spherical formation (with sizes up to 2.23 μm in N and 3.03 μm in T) can be observed, with a rigid surface, whereas a double microencapsulation can be suggested in sample T (Fig. 3, b). These structural and morphological particularities are essential in determining the profile of the controlled release of bioactive compounds.
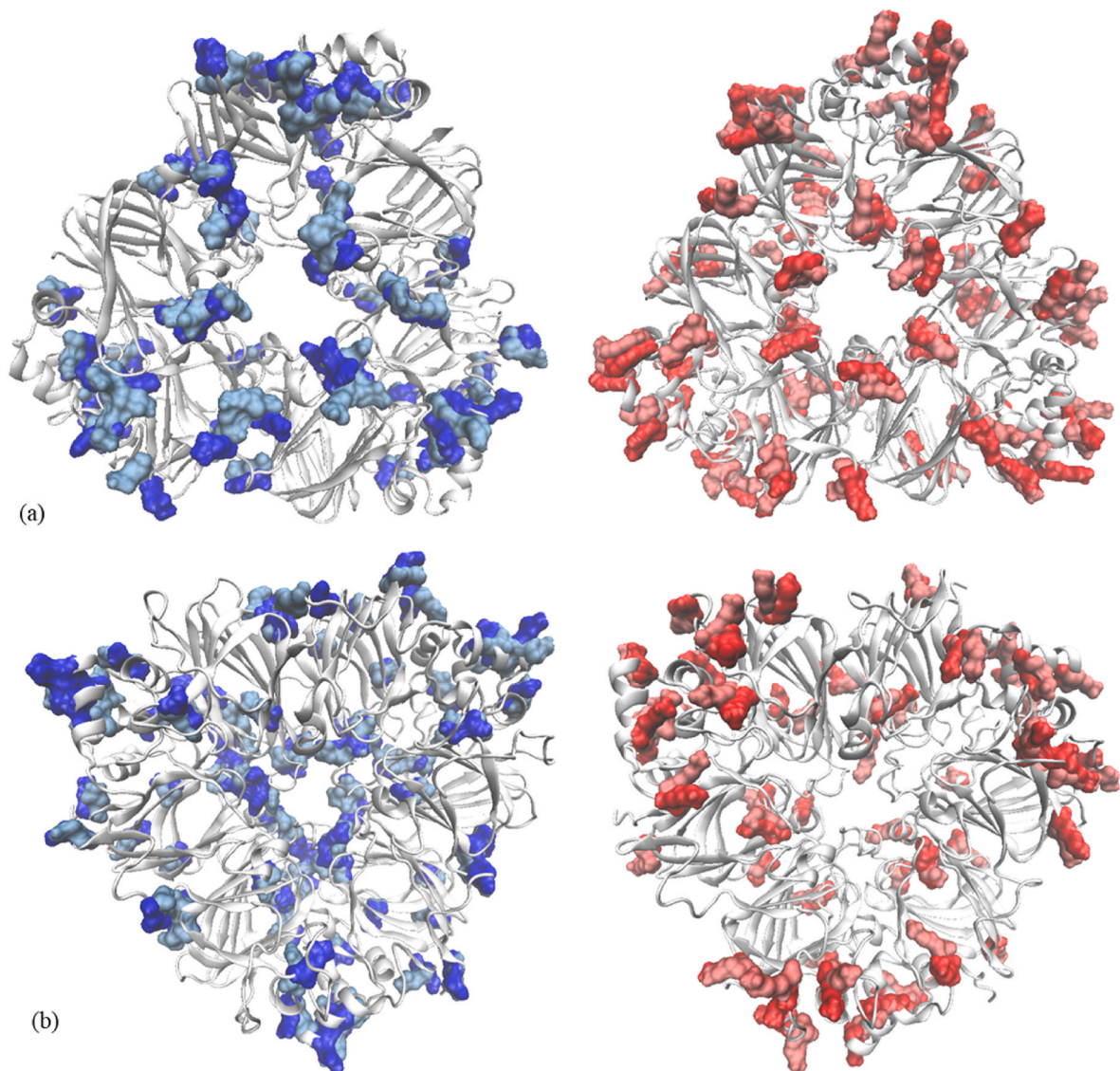
Fig. 2. Superposition of the main soy proteins equilibrated at different temperatures: (a) 7S and (b) 11S molecules. In the models equilibrated at 50 °C, Gln and Lys residues are highlighted in blue and red, respectively. In the models equilibrated at 85 °C, Gln and Lys residues are highlighted in brushed metal blue and red, respectively. (For interpretation of the references to color in this figure legend, the reader is referred to the Web version of this article.)

4. Conclusions

In this study, the co-solvent assisted supercritical CO_2 extraction of rosehip fruits allowed to obtain two extracts, with unique phytochemical profiles, thus tuning the opportunities to extract different compounds, such as complex oleoresins containing polyphenols, carotenoids, oils, phytosterols, tocopherols, etc. The SFE extraction in two separators, allowed to obtain a S40 fraction enriched in fatty acids and a S45 fraction with a higher content in (+)-catechin, β-cryptoxanthin, β-carotene, α- and γ-tocopherols, and β-sitosterol. Due to the significant fatty acids and carotenoid contents, the S40 oleoresins were microencapsulated in two customized matrices, based on one- and two steps cross-linking mediated reactions of soy protein isolates. The one-step cross-linked powder showed a higher concentration in bioactive, excepting palmitoleic acid, allowing to obtain o higher antioxidant activity. Molecular modelling investigations targeting the main soy proteins revealed that the heating step, applied for obtaining the two-step cross-linked powder, caused significant reduction of the exposure of some Gln residues, involved in the transglutaminase assisted cross-linking reactions. The microparticles displayed spherical formations,

smaller and more abundant in one-step cross-linked powder, with a rigid surface. A possible double microencapsulation was suggested for the two-step cross-linked powder, which can be associated with a greater protective effect of the customized wall matrices on bioactive release. Our study proved that cross-linked aggregates mediated by transglutaminase applied for microencapsulation of rosehip oleoresins may be a promising method to deliver functional powders. Further studies are needed in order to test the potential functional properties of both free extracts and microparticles, such as the ability to inhibit selected metabolic syndrome associated enzymes, anti-inflammatory and antimicrobial activities, etc. Additionally, further studies aiming to advance the microencapsulation potential of both individual and cumulative supercritical fluids extraction associated fractions into functional powders are currently developed in our laboratories.

Funding
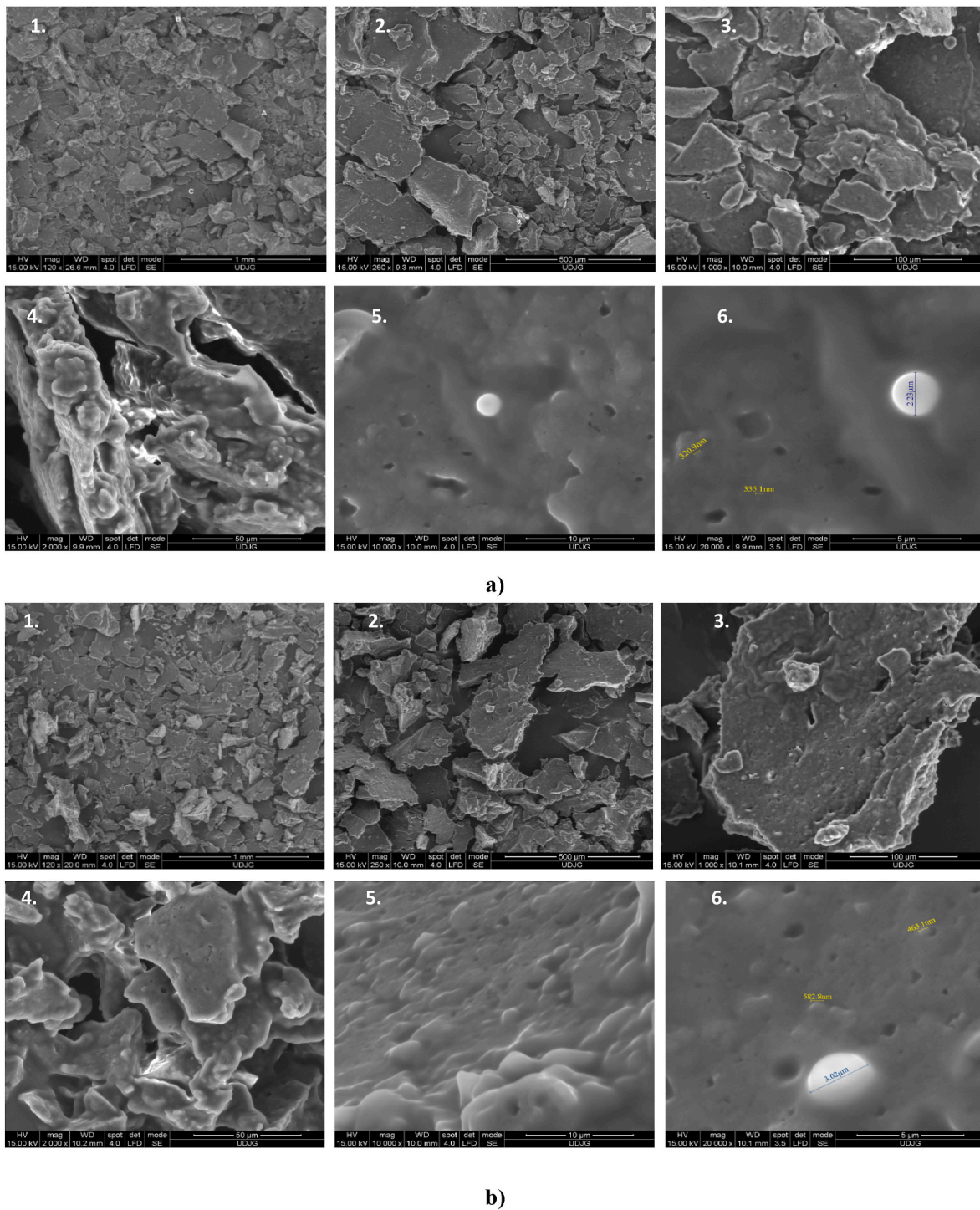
Fig. 3. Scanning electron micrographs of microencapsulated oleoresins from rosehip fruits in one-step cross-linked soy protein isolates (a) and two step cross-linked soy protein isolates (b) at different magnification of 120 × (1), 250 × (2), 1000 × (3), 2000 × (4), 10 000 × (5) and 20 000 × (6).

Institutional review board statement

Not applicable.

Informed consent statement

Not applicable.

CRediT authorship contribution statement

Liliana Mihalcea: Conceptualization, Methodology, Formal analysis, Resources, Writing – original draft, preparation, Writing – review & editing, Visualization, Supervision, Project administration, Funding acquisition, All authors have read and agreed to the published version of the manuscript. **Bogdan Păcularu-Burada:** Formal analysis, All authors have read and agreed to the published version of the manuscript. **Ște-fania-Adelina Milea:** Methodology, Formal analysis, Writing – original draft, preparation, All authors have read and agreed to the published

version of the manuscript. **Iuliana Aprodu:** Writing – review & editing, Methodology, Software, Formal analysis, All authors have read and agreed to the published version of the manuscript. **Nina-Nicoleta Condurache (Lazăr):** Methodology, Formal analysis, Writing – original draft, preparation, All authors have read and agreed to the published version of the manuscript. **Elena Iulia Cucolea:** Formal analysis, All authors have read and agreed to the published version of the manuscript. **George-Mădălin Dănilă:** Formal analysis, All authors have read and agreed to the published version of the manuscript. **Adrian Cîrciumaru:** Formal analysis, All authors have read and agreed to the published version of the manuscript. **Stănciuc Nicoleta:** Conceptualization, Methodology, Software, Writing – original draft, preparation, Writing – review & editing, Visualization, Supervision, Funding acquisition, All authors have read and agreed to the published version of the manuscript.

Declaration of competing interest

The authors declare that they have no known competing financial interests or personal relationships that could have appeared to influence the work reported in this paper.

Data availability

Data will be made available on request.

Acknowledgments

References

Abraham, M.J., Murtola, T., Schulz, R., Páll, S., Smith, J.C., Hess, B., Lindahl, E., 2015. GROMACS: high performance molecular simulations through multi-level parallelism from laptops to supercomputers. SoftwareX 1, 19–25.

Adachi, M., Takenaka, Y., Gidamis, A.B., Mikami, B., Utsumi, S., 2001. Crystal structure of soybean proglycinin A1aB1b homotrimer. J. Mol. Biol. 305 (2), 291–305.

Alavarse, A.C., Frachini, E.C.G., da Silva, R.L.C.G., Lima, V.H., Shavandi, A., Petri, D.F.S., 2022. Crosslinkers for polysaccharides and proteins: synthesis conditions, mechanisms, and crosslinking efficiency. Int. J. Biol. Macromol. 202, 558–596.

Antoniolli, A., Fontana, A.R., Piccoli, P., Bottini, R., 2015. Characterization of polyphenols and evaluation of antioxidant capacity in grape pomace of the cv. Malbec. Food Chem. 178, 172–178.

AOAC, 1998. Official Methods of Analysis. Association of Analytical Chemist, Airlington, USA.

Batista, R.A., Espiti, P.J.P., de Souza Siqueira Quintans, J., Freitas, M.M., Cerqueir, M.A., Teixeira, J.A., Cordeiro Cardoso, J., 2019. Hydrogel as an alternative structure for food packaging systems. Carbohydr. Polym. 205, 106–116.

Can-Cauich, C.A., Sauri-Duch, E., Moo-Huchin, V.M., Betancur-Ancona, D., Cuevas-Glory, L.F., 2019. Effect of extraction method and specie on the content of bioactive compounds and antioxidant activity of pumpkin oil from Yucatan, Mexico. Food Chem. 285, 186–193.

de Santana, F.B., Caixeta Gontijo, L., Mitsutake, H., Mazivila, S.J., de Souza, L.M., Borges Neto, W., 2016. Non-destructive fraud detection in rosehip oil by MIR spectroscopy and chemometrics. Food Chem. 209, 228–233.

Dumitrașcu, L., Stănciuc, N., Grigore-Gurgu, L., Aprodu, I., 2020. Investigation on the interaction of heated soy proteins with anthocyanins from cornelian cherry fruits. Spectrochim. Acta Mol. Biomol. Spectrosc. 231, 118114.

Duru, N., Karadeniz, F., Erge, H.S., 2011. Changes in bioactive compounds, antioxidant activity and HMF formation in rosehip nectars during storage. Food Bioprocess Technol. 5, 2899–2907.

Erenturk, S., Gulaboglu, M.S., Gultekin, S., 2010. Experimental determination of effective moisture diffusivities of whole- and cut-rosehips in convective drying. Food Bioprod. Process. 88 (2), 99–104.

Franco, D., Sineiro, J., Pinelo, M., Núñez, M.J., 2007. Ethanolic extraction of Rosa rubiginosa soluble substances: oil solubility equilibria and kinetic studies. J. Food Eng. 79 (1), 150–157.

Goztepe, B., Kayacan, S., Bozkurt, F., Tomas, M., Sagdic, O., Karasu, S., 2022. Drying kinetics, total bioactive compounds, antioxidant activity, phenolic profile, lycopene and β-carotene content and color quality of Rosehip dehydrated by different methods. LWT 156, 112476.

Hoare, T.R., Kohane, D.S., 2008. Hydrogels in drug delivery: progress and challenges. Polymer 49, 1993–2007.

Horvath, G., Molnar, P., Rado-Turcsi, E., Deli, J., Kawase, M., Satoh, K., Molnar, J., 2012. Carotenoid composition and *in vitro* pharmacological activity of rose hips. Acta Biochim. Pol. 59 (1), 129–132.

Igual, M., Chis, M.S., Păucean, A., Vodnar, D.C., Ranga, F., Mihăiescu, T., Martínez-Monzó, J., García-Segovia, P., 2021. Effect on nutritional and functional characteristics by encapsulating *Rose canina* powder in enriched corn extrudates. Foods 10, 2401.

Igual, M., García-Herrera, P., Cámara, R.M., Martínez-Monzó, J., García-Segovia, P., Cámara, M., 2022. Bioactive compounds in rosehip (*Rosa canina*) powder with encapsulating agents. Molecules 27, 4737.

İlyaso-ğlu, H., 2014. Characterization of rosehip (*Rosa canina* L.) seed and seed oil. *Int.* J. Food Prop. 14, 1591–1598.

Jahongir, H., Zhang, M., Amankeldi, I., Yu, Z., Changheng, L., 2019. The influence of particle size on supercritical extraction of dog rose (Rosa canina) seed oilJ. In: Eng. Sci., 31 King Saud Univ, pp. 140–143.

Koch, J.A., Bolderdijk, J.W., van Ittersum, K., 2021. Disgusting? No, just deviating from internalized norms. Understanding consumer skepticism toward sustainable food alternatives. J. Environ. Psychol. 76, 101645.

Li, H., Zhu, K., Zhou, H., Peng, W., 2012. Effects of high hydrostatic pressure treatment on allergenicity and structural properties of soybean protein isolate for infant formula. Food Chem. 132, 808–814.

Machmudah, S., Kawahito, Y., Sasaki, M., Goto, M., 2007. Supercritical CO_2 extraction of rosehip seed oil: fatty acids composition and process optimization. J. Supercrit. Fluids 41, 421–428.

Machmudah, S., Kawahito, Y., Sasaki, M., Goto, M., 2008. Process optimization and extraction rate analysis of carotenoids extraction from rosehip fruit using supercritical CO_2. J. Supercrit. Fluids 44 (3), 308–314.

Maruyama, N., Adachi, M., Takahashi, K., Yagasaki, K., Kohno, M., Takenaka, Y., Okuda, E., Nakagawa, S., Mikami, B., Utsumi, S., 2001. Crystal structures of recombinant and native soybean β-conglycinin β homotrimers. Eur. J. Biochem. 268 (12), 3595–3604.

Maruyama, Y., Maruyama, N., Mikami, B., Utsumi, S., 2004. Structure of the core region of the soybean β-conglycinin α' subunit. Acta Crystallogr. D Biol. Crystallogr. 60 (2), 289–297.

Medveckienė, B., Kulaitienė, J., Jarienė, E., Vaitkevičienė, N., Hallman, E., 2020. Carotenoids, polyphenols, and ascorbic acid in organic rosehips (*Rosa* spp.) cultivated in Lithuania. Appl. Sci. 10 (15), 5337.

Mihalcea, L., Crăciunescu, O., Gheonea, I., Prelipcean, A.M., Enachi, E., Barbu, V., Bahrim, G.E., Râpeanu, G., Oancea, A., Stănciuc, N., 2021. Supercritical CO_2 extraction and microencapsulation of lycopene-enriched oleoresins from tomato peels: evidence on antiproliferative and cytocompatibility activities. Antioxidants 10 (2), 1–15.

Mihalcea, L., Turturică, M., Barbu, V., Ionita, E., Pătrașcu, L., Cotârleț, M., Dumitrașcu, L., Aprodu, I., Râpeanu, G., Stănciuc, N., 2018. Transglutaminase mediated microencapsulation of sea buckthorn supercritical CO_2 extract in whey protein isolate and valorization in highly value-added food products. Food Chem. 262, 30–38.

Neagu, C., Mihalcea, L., Enachi, E., Barbu, V., Borda, D., Bahrim, G.E., Stănciuc, N., 2020. Cross-linked microencapsulation of CO_2 supercritical extracted oleoresins from sea buckthorn: evidence of targeted functionality and stability. Molecules 25, 2442.

Nesterenko, A., Alric, I., Silvestre, F., Durrieu, V., 2013. Vegetable proteins in microencapsulation: a review of recent interventions and their effectiveness. Ind. Crop. Prod. 42, 469–479.

Ouerghemmi, S., Sebei, H., Siracusa, L., Ruberto, G., Saija, A., Cimino, F., Cristani, M., 2016. Comparative study of phenolic composition and antioxidant activity of leaf extracts from three wild *Rosa* species grown in different Tunisia regions: *Rosa canina* L., *Rosa moschata* herrm. and *Rosa sempervirens* L. Ind. Crop. Prod. 94, 167–177.

Özdemir, N., Pashazadeh, H., Zannou, O., Koca, I., 2022. Phytochemical content, and antioxidant activity, and volatile compounds associated with the aromatic property, of the vinegar produced from rosehip fruit (*Rosa canina* L.). LWT 154, 112716.

Roman, D., Condurache, N.N., Aprodu, I., Enachi, E., Barbu, V., Bahrim, G.E., Stănciuc, N., Râpeanu, G., 2021. Insights of sea buckthorn extract's encapsulation by coacervation technique. Inventions 6, 59.

Salgın, U., Salgın, S., Ekici, D.D., Uludağ, Y., 2016. Oil recovery in rosehip seeds from food plant waste products using supercritical CO_2 extraction. J. Supercrit. Fluids 118, 194–202.

Sernaite, L., Urbonaviciene, D., Bobinas, C., Viskelis, P., 2019. Optimisation of Supercritical Carbon Dioxide Extraction of Lipophilic Extract from Rosehips. Foodbalt, pp. 188–192.

Taneva, I., Petkova, N., Dimov, I., Ivanov, I., Denev, P., 2016. Characterization of rose hip (*Rosa canina* L.) fruits extracts and evaluation of their *in vitro* antioxidant activity. J. Pharmacogn. Phytochem. 5 (2), 35–38.

Vidović, S., Vladić, J., Nastić, N., Jokić, S., 2021. Subcritical and supercritical extraction in food by-product and food waste valorization. Ref. Modul. Food Sci. 705–721.

Zuknik, M.H., Norulaini, N.N., Omar, A.K.M., 2012. Supercritical carbon dioxide extraction of lycopene: a review. J. Food Eng. 112 (4), 253–262.